Journal of Power Sources 183 (2008) 310–315

Contents lists available at ScienceDirect

Journal of Power Sources

journal homepage: www.elsevier.com/locate/jpowsour

A high energy Li-ion battery based on nanosized $LiNi_{0.5}Mn_{1.5}O_4$ cathode material

José C. Arrebola, Alvaro Caballero, Lourdes Hernán*, Julián Morales

Departamento de Química Inorgánica e Ingeniería Química, Universidad de Córdoba, Edificio Marie Curie, Campus de Rabanales, 14071 Córdoba, Spain

ARTICLE INFO

Article history:
Received 22 January 2008
Received in revised form 4 March 2008
Accepted 9 April 2008
Available online 22 April 2008

Keywords:
Nanometric spinel
High voltage
Lithium batteries
MCMB

ABSTRACT

The electrochemical performance of a Li-ion battery made from nanometric, highly crystalline $LiNi_{0.5}Mn_{1.5}O_4$ as positive electrode and mesoporous carbon microbeads (MCMBs) as negative electrode was assessed. The best performance was obtained by using a slight excess of spinel (a cathode/anode mole ratio of 1.3) and lithium bis-oxalate borate (LiBOB) instead of $LiPF_6$ as an electrolyte salt. Higher spinel contents caused the formation of metallic Li in the carbon and the rapid degradation of battery performance as a result. The calculated output energy was 322 Wh kg^{-1} which is higher than the value reported for the $LiMn_2O_4$/C cell (250 Wh kg^{-1}).

1. Introduction

Rechargeable lithium-ion (Li-ion) batteries are part in the so-called "advanced battery technology", which provides significant advantages in performance over Ni-based technologies. For example, Li-ion technology provides three to four times higher gravimetric and volumetric energy densities, and voltages more than three times higher than the typical levels for Ni-based battery systems.

Lithium-ion batteries use carbon/graphite rather than metallic lithium as an anode. The theoretical capacity of graphite is 372 mAh g^{-1} special attention in this context has been paid to mesocarbon microbeads (MCMBs), which possess a graphite-based structure [1,2] and a stable lithium intercalation capacity of 325 mAh g^{-1} [3]. Also, $LiCoO_2$ is the most commonly used cathodic material. Batteries constructed from these materials provide an average voltage of 3.5 V. This Li compound has two widely accepted shortcomings, namely: its toxic character and its high cost. For this reason, although many alternative compounds have been tested as materials for half-cells, few have been tested in Li-ion cell configurations with the exception of $LiMn_2O_4$ and, more recently, $LiFePO_4$. The former compound was first studied by Tarascon and Guyomard [4]. Recently, Amine and coworkers [5,6] and Sano et al. [7] revisited its electrochemical behavior at high temperatures. Our group has assessed its performance against $Li_4Ti_5O_{12}$ as an anode [8] and found particles of nanometric size to have a beneficial effect. Most studies in this context have been performed with $LiPF_6$ dissolved in organic solvents as electrolyte. This inorganic salt can release HF in the presence of water traces. Its high reactivity detracts from battery performance and its deleterious effects are believed to be boosted in the presence of Mn^{3+} ion [9]; this tends to disproportionate into Mn^{2+} and Mn^{4+}, the former ion being easily transferred to the organic solvent. This shortcoming can be circumvented by using LiBOB instead of $LiPF_6$ [10–12].

$LiNi_{0.5}Mn_{1.5}O_4$ (LNMO) is one alternative spinel formally free of Mn^{3+} the electrochemical properties of which in Li half-cells have been extensively studied and confirmed to be quite good [13–17]. This spinel can provide potentials higher than those of $LiMn_2O_4$ (4.7 V vs. 4.2 V referred to Li^+/Li electrode), which can facilitate the development of a new battery generation of higher energy. Recently, the Li–Ni–Mn spinel was studied in Li-ion cells using graphite [18], tin electroplated [19] and TiO_2(B) [20] as anodes. In this work we examined the electrochemical properties of this spinel in hybrid batteries using MCMB as an anode. The spinel was synthesized as highly crystalline nanometric particles possessing an excellent rate capability in Li half-cells [16]. Following a brief description of the electrochemical behavior of the two systems versus Li, the electrochemical properties of LNMO/MCMB cells are discussed with special emphasis on the factors most markedly influencing cell performance (e.g. the cathode/anode material weight ratio and nature of the electrolyte).

2. Experimental

MCMB was supplied by Osaka Gas in particle sizes ranging from 5 to 8 μm and a specific surface area of 4 m^2 g^{-1}. The synthesis,

* Corresponding author. Tel.: +34 957 218620; fax: +34 957 218621.
E-mail address: iq1hepal@uco.es (L. Hernán).

0378-7753/$ – see front matter © 2008 Elsevier B.V. All rights reserved.
doi:10.1016/j.jpowsour.2008.04.036

Table 1
Irreversible capacity (mAh g^{-1}) at variable charge/discharge rates (C is referred to 1 Li^+ exchanged in 1 h, equivalent to 372 mAh g^{-1})

C/20	55
2C	55
5C	33

Electrolyte: 1 M $LiPF_6$ in EC:DMC.

and the textural and structural properties, of LNMO spinel are described in detail elsewhere (sample named PEG-800) [16]. This is a suitable grinding-based method for synthesizing highly crystalline nanoparticles [21,22]. Each active material was mixed with 10% polyvinylidene fluoride (PVDF) and 5% carbon black (Super P). These mixtures were used to prepare the electrodes by forming a slurry in *N*-methyl-2-pyrrolydone and spreading it onto copper (anode) and aluminum (cathode) foils using the doctor blade technique.

Electrochemical measurements were performed on two- (CR2032 coin type) and three-electrode (Toyo System) cells. The latter cell type was used to monitor the potential of the LNMO/MCMB, LNMO/Li and MCMB/Li redox couples simultaneously. Two different electrolytes were used, namely: 1 M anhydrous $LiPF_6$ in a 1:1 (w/w) mixture of ethylene carbonate (EC) and dimethylcarbonate (DMC), supplied by Hohsen, and 1 M LiBOB (supplied by Chemetall GbmH) dissolved in the same solvents. According to Xu et al. [12] LiBOB has comparable anodic stability with $LiPF_6$. Recently, Wang et al. [23] have confirmed its electrochemical stability up to 5 V versus Li^+/Li, and Yu et al. [24] have confirmed the greater stability of LiBOB EC/EMC/DEC (1:1:1) compared with $LiPF_6$ EC/EMC/DEC (1:1:1) at voltages higher than 4.5 V. This justifies the selection of this salt for use in our high voltage lithium-ion batteries. Cycling tests were performed on an Arbin BT2000 potentiostat–galvanostat system under a galvanostatic regime, using the following voltage windows: MCMB/Li (0.0–1.5 V), LNMO/Li (3.5–4.95) and LNMO/MCMB (3.5–4.85). The choice of the last window was based on a combination of the half-cell reaction voltage. Because the reaction of MCMB with Li occurs over the 0.05–0.1 V range, we subtracted this value from the limits of the LNMO/Li half-cell with the aim to avoid unwanted reactions. The specific capacities and rates of the Li-ion batteries given here are referred to the mass of the negative electrode.

3. Results and discussion

3.1. Electrochemical properties of MCMB versus Li

MCMB is a commercially available, widely studied graphite-based carbon material. For this reason, we briefly describe its electrochemical properties towards Li with two main purposes, namely: (i) to determine its irreversible capacity and (ii) to assess its rate capability over a wide range of current densities. The irreversible capacity will be an useful parameter with a view to more accurately determine the cathode/anode ratio for the Li-ion cells in order to optimize their operating conditions. The irreversible capacity determined from the difference between the first and second discharge is shown in Table 1. As can be seen, the irreversible capacity hardly changed from C/20 to 2C and was somewhat smaller at 5C.

The cycling properties of the half-cell over the first 50 cycles are illustrated in Fig. 1. In order to facilitate understanding of the influence of the rate on the specific capacity, Table 2 shows some selected values obtained in the 2nd, 50th and 100th cycle. As commonly observed in the second cycle, the capacity decreased as the discharge/charge rate increased. The decrease was particularly

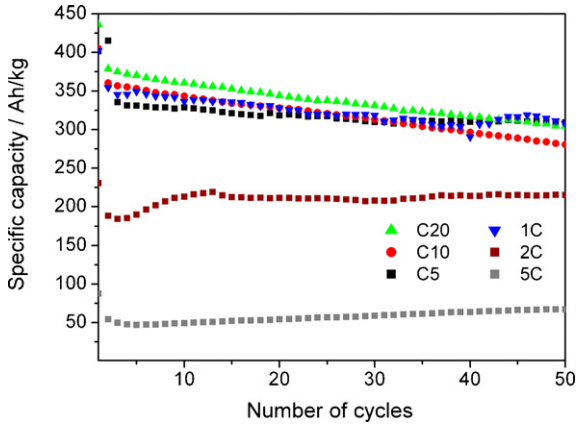

Fig. 1. Variation of the specific capacity of the MCMB/Li half-cell as a function of the number of cycles at variable rates. Electrolyte: 1 M $LiPF_6$ in EC:DEC.

marked at high rates (2C and 5C). This simply reflected the fact that the micrometric size of the particles hindered lithium diffusion and the particles were unable to respond to such high current densities. Whichever the rate, the capacity faded on cycling, being somewhat more pronounced at the lowest rates (C/20 and C/10). Although the capacity retention with cycling was quite good at higher rates (2C and 5C), the capacity was considerably reduced. In conclusion, the best rate capabilities of this MCMB for Li-ion batteries in terms of delivered capacity and capacity retention were those obtained at C/5 and 1C, which were thus chosen to study the LNMO/MCMB system.

3.2. Electrochemical properties of LNMO versus Li

As stated above, $LiNi_{0.5}Mn_{1.5}O_4$ was prepared as highly crystalline nanometric particles. The use of nanometric materials to construct electrodes for lithium-ion batteries has aroused much interest recently [25,26]. Trivial size effects (e.g. an increased surface-to-volume ratio and shorter length displacements for Li^+ ions) can help to improve the rate capability and cycle life of cells. By contrast, the large surface area of the electrode and electrode/electrolyte interface provide additional advantages for nanometric particles coating the bulk material [27] such as (i) an improved reaction kinetics that reflects in increased development and reversibility of the lithium insertion/extraction process, which improve cell capacity and capacity retention; (ii) the ability to use high charge/discharge rates.

Based on the foregoing, the electrochemical behavior of the spinel versus Li was tested from C/4 to 8C; no lower charge/discharge rates were used as they strongly deteriorate nanoparticle-based electrodes upon cycling [28]. The discharge capacity delivered by the spinel was quite similar (Fig. 2); thus, it ranged from 140 mAh g^{-1} at 1C to 115 mAh g^{-1} at 8C, and faded slowly on cycling. Fading was slightly more marked at the lowest rate (C/4). As noted earlier, the increased slope of the capacity

Table 2
Specific discharge capacity of MCMB/Li half-cells at variable rates (C/20 to 1C). Electrolyte: 1M $LiPF_6$ in EC:DMC

Rate	Cycle		
	2nd	50th	100th
C20	375.2	304.0	257.0
C10	356.8	280.8	225.0
C5	351.6	309.4	280.0
1C	345.2	307.7	276.0

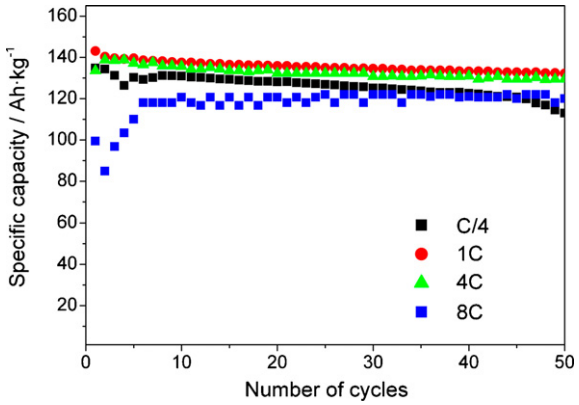

Fig. 2. Variation of the specific capacity of the LNMO/Li half-cell as a function of the number of cycles at variable rates. Electrolyte: 1 M $LiPF_6$ in EC:DMC.

versus cycle number plot at low rates is a common finding for nanometric cathodic materials and probably results from a combination of an increased reactivity towards the electrolyte and prolonged contact between the active material and electrolyte. In any case, this nanometric spinel exhibits a good electrochemical response in terms of both capacity and cycling properties over a wide range of rate capabilities. Performance was optimal at 1C. Under this regime, the average delivered capacity exceeded 135 mAh g^{-1} and was close to the calculated value obtained from the spinel formula (148 mAh g^{-1}).

3.3. Electrochemical properties of LNMO/MCMB cells

Once the charge/discharge rate for both materials was optimized, we focused on the cathode/anode ratio in order to maximize the delivered capacity and capacity retention. To this end, we used three cathode/anode ratios, namely: 1.3, 1.6 and 2 moles of LNMO per C_6. Referred to the capacity ratio of the negative electrode (N) to the positive electrode (P) (N/P ratio), these values are equivalent to 0.73, 0.59 and 0.47, respectively. These values were calculated by using average specific capacities obtained from the data of Figs. 1 and 2, 320 and 135 mAh g^{-1} for MCMB and LNMO, respectively. Although the ideal N/P ratio should be 1.0 [28], values range from 0.45 to 1.49 are used by different manufactures [29]. Fig. 3a shows the variation of the capacity as a function of the number of cycles. Although the highest capacity was that delivered by the cell made in a mole ratio of 2 (400 mAh g^{-1}), it rapidly faded on cycling, particularly over the first 10 cycles. After 40 cycles, the capacity of the three cells was quite similar (around 100 mAh g^{-1}). There was thus a significant loss of capacity on cycling. A similar behavior was previously observed by Chen et al. [30] for $LiMn_2O_4$–MCMB cells. The poor capacity retention was ascribed to attack by the electrolyte and its partial dissolution in the organic solvent, otherwise facilitated by the presence of tervalent Mn [9]. It seems rather plausible that a small amount of Mn^{3+} may be present in the spinel framework by effect of some Ni defect or the presence of tervalent Ni. However, there contradicts the fact that the phenomenon was apparently absent when the spinel was cycled versus Li. The suggestion that this chemical reaction allows manganese ions to migrate from the positive electrode to the negative electrode if made from graphite [30] requires experimental confirmation.

In order to overcome this problem, measurements were repeated by using LiBOB as electrolyte. Fig. 3b shows the variation of the discharge values as a function of the number of cycles for the four cells tested (from 1.0 to 2.0 mole ratio). The cells made at the two limiting ratios also delivered the two extreme capacity values (viz. 450 and 170 mAh g^{-1} at a mole ratio of 2 and 1, respectively). The other ratios gave intermediate values (around 330 mAh g^{-1}). Note the increased capacity retention of the cells relative to that obtained with $LiPF_6$ as an electrolyte irrespective of the particular mole ratio used. It has been suggested that LiBOB protects the anode more efficiently than does $LiPF_6$. This is a result of the formation of a stronger SEI (solid electrolyte interface) that hinders Mn metal deposition on surface of the negative electrode. Besides, the amount of dissolved Mn should be lower because LiBOB is less reactive than $LiPF_6$ towards Li. For this reason, the cells using LiBOB as electrolyte deteriorate more slowly than those using LPF_6 [30,31]. Indirect evidence of LiBOB decomposition and subsequent film formation on MCMB was obtained from the shape of the charge/discharge curves of Fig. 4. On charging, the cell exhibited not only its major electrochemical peaks above 4.5 V, due to Li extraction from the spinel and its insertion into the graphite structure – which is studied in greater detail below – but also a small pseudoplateau at ca. 2.2 V which can be ascribed to the formation of an SEI on the carbon electrode and appears as a peak at 1.78 V versus Li (a value consistent with the reduction process of LiBOB [32]) in the differential capacity plot (see the inset of Fig. 4). This peak is only observed on the first cathodic polarization of graphite electrode, which is indicative of its irreversible nature. The remaining plateaux, assigned to Li transfer from the cathode to the anode and *vice versa*, retain their main characteristics (particularly their voltages) on cycling, consistent with the reversible nature of the electrochemical reaction.

Again, the highest mole ratio gave the worse results and the capacity in the 40th cycle was only 100 mAh g^{-1} (22% of the initial capacity). The cell exhibiting the best capacity retention was that

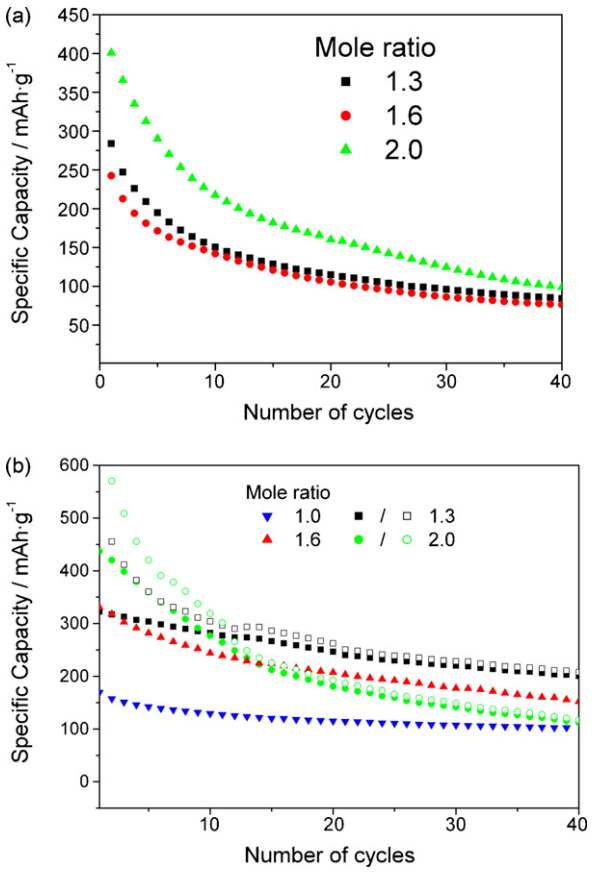

Fig. 3. Variation of the capacity delivered by the LNMO/MCMB Li-ion cells as a function of the number of cycles, using (a) $LiPF_6$ and (b) LiBOB as electrolyte. Full symbols represent discharge values and empty symbols represent charge values. Tests were carried out at C/4.

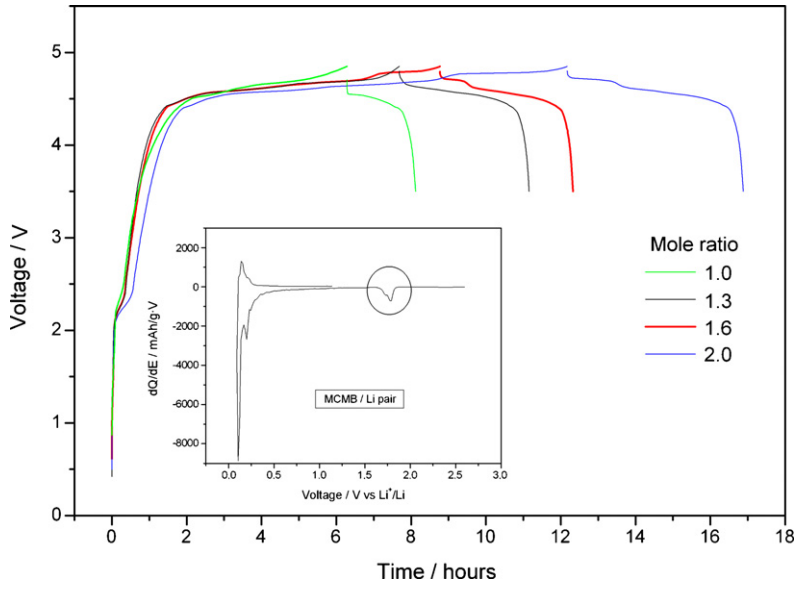

Fig. 4. First charge/discharge curves recorded at C/4 for the LNMO/MCMB pair. The inset shows the differential capacity plot for the MCMB/Li pair (mole ratio 1.3). All measurements were made in a three-electrode cell. Electrolyte: 1 M LiBOB in EC:DMC.

made in a mole ratio of 1, which retained 74% of its initial capacity after the 40th cycle. However, its initial capacity was rather low (170 mAh g^{-1}). The best performance in terms of both delivered capacity and capacity retention was that of the cell made in a 1.3 mole ratio. This result is interesting, in as much the excess of cathodic material needed to obtain a good electrochemical response is small. Moreover, the effective energy of our cell as calculated with provision for both the positive and the negative active material was 325 Wh kg^{-1} (i.e. 1.30 times greater than that obtained with the $LiMn_2O_4$/carbon cell) [4].

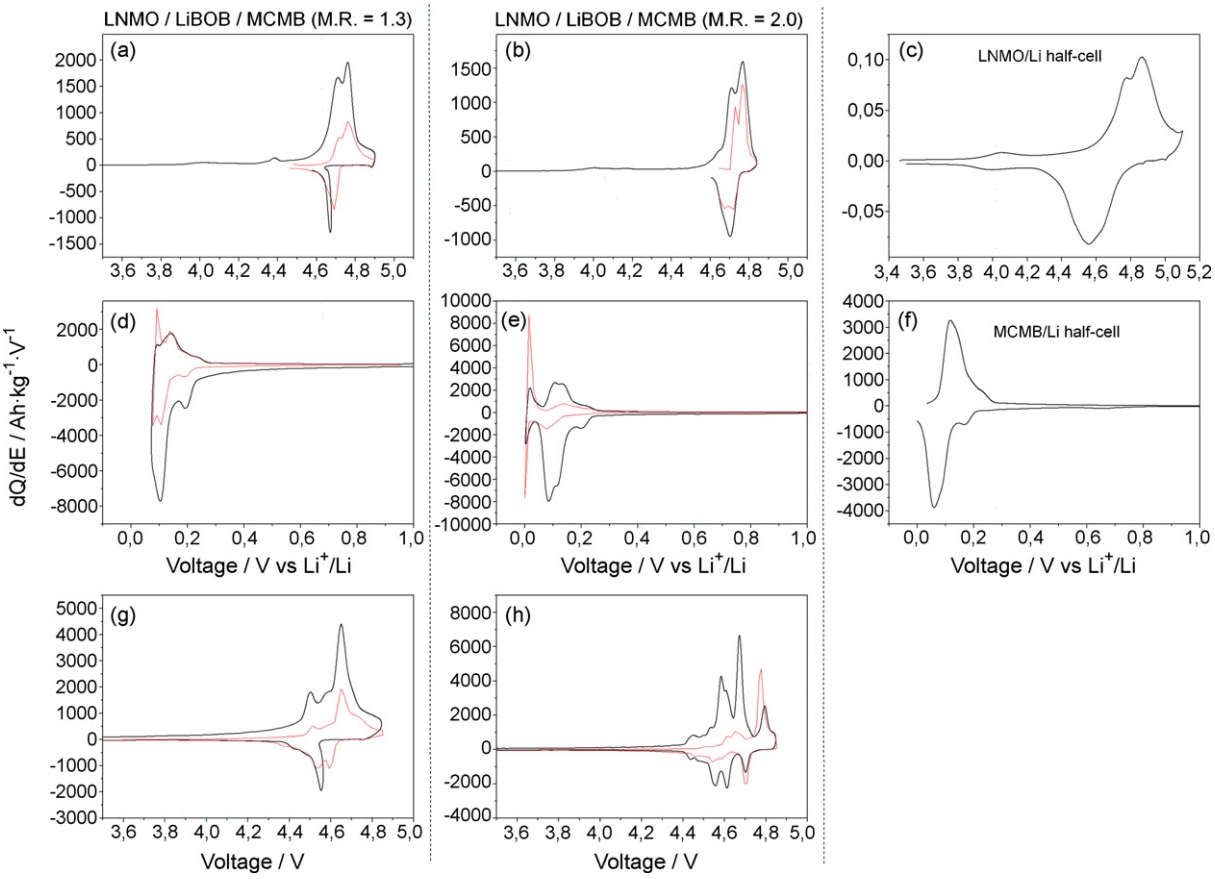

Fig. 5. dQ/dE plots for LNMO/LiBOB/MCMB three-electrode cells obtained at MR = 1.3 (a, d and g) and MR = 2.0 (b, e and h). For comparison, the results obtained with LNMO/Li (c) and MCMB/Li half-cells (f) are also shown. Black and red lines, first and tenth cycles, respectively. (For interpretation of the references to color in this figure legend, the reader is referred to the web version of the article.)

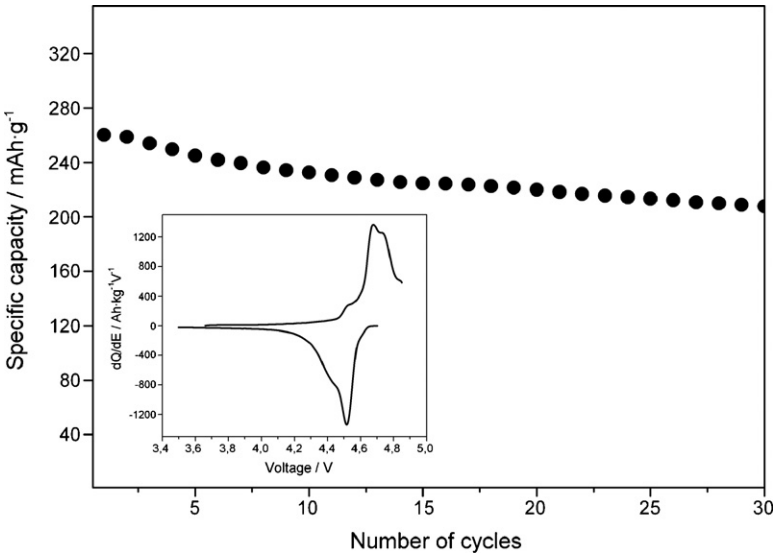

Fig. 6. Variation of the capacity delivered by the LNMO/LiBOB/MCMB Li-ion cells as a function of the number of cycles. Cycling rate: 1C. The inset shows the dQ/dE plot for the first cycle.

These results raise the following question: why, if the mole ratio ranged from 1.6 to 2, capacity retention was rather poor even though the capacity delivered by the cell was quite high? In order to shed some light on this question, we have included in Fig. 3b the values of the charge process for the best and worst performing cell (mole ratio 1.3 and 2, respectively). The outcome was quite similar: an overcharge after the first few cycles. Thus, after 10 cycles, the discharge and charge capacity values tended to converge, and the coulombic efficiency approached 100%. Therefore, these results are of not use to assess the performance of the cells and clarify the origin of the capacity fading.

More illustrative were the results obtained with a three-electrode Li-ion cell with metallic lithium as a reference electrode and assembled to three independent testing channels. The system allowed us to simultaneously record the cell voltage (E cell), the potential of the anode [$E_{(-)}$] and that of the cathode [$E_{(+)}$]. Fig. 5 shows the galvanostatic curves plotted in the form of differential capacities (dQ/dV) used to identify the electrochemical reactions as peaks, equivalent to the pseudoplateaux in the charge/discharge curves (Fig. 4). The curves were recorded for the electrodes made in the mole ratios 1.3 (i.e. the best-performing cell) and 2.0 (the worst-performing cell) in the 1st and 10th cycle—where the capacity significantly faded in the latter cell.

As can be seen, the shape of the differential capacity plot for the LNMO/Li half-cell coincided with that expected for this spinel irrespective of the cathode/anode ratio and extent of cycling (Fig. 5a and b). For comparison, the differential capacity plot for the same half-cell, albeit in two-electrode configuration, is also shown (Fig. 5c). On charging, a double peak appeared at 4.7–5.0 V consistent with lithium removal via two cubic/cubic two-phase reactions [33] and subsequent oxidation of Ni^{2+} to Ni^{4+} [34]. The peak was also observed on discharging to a somewhat lower voltage, which testifies the good reversibility of this electrode. By contrast, the shape of the differential capacity plot for the MCMB/Li half-cell was influenced by the cathode/anode ratio (Fig. 5d and e). For comparison, the figure includes the galvanostatic charge/discharge curves for the MCMB/Li half-cell in the two-electrode configuration (Fig. 5f). On intercalating lithium, the electrode made in a 1.3 mole ratio exhibited three major peaks at 0.2, 0.1 and 0.07 V, consistent with earlier reports [1,2]. This shape was virtually retained by the three-electrode configuration for the first cycle (Fig. 5d). However, the electrode made in a 2 mole ratio, clearly exhibited a new peak close to 0 V (Fig. 5e). As suggested by the peak observed at 0.02 on deintercalating the cell, the reaction responsible for this signal is reversible. Before we address the origin of this peak, we should note the shape of differential capacity plot for the LNMO/MCMB cell. The cell made in a mole ratio of 2.0 (Fig. 5h) exhibited a more complex profile that that made in a 1.3 mole ratio (Fig. 5g). On charging the cell, a third peak was observed above 4.8 V in addition to the two major peaks describing lithium extraction. This peak had its counterpart on the discharging curve at ca. 4.7 V. These peaks clearly appear as the higher voltage pseudoplateau in both the charge and the discharge curves for the electrodes made in a 1.6 and 2.0 mole ratio; also, their length increases as the spinel content increases (see Fig. 4).

The comments made on the differential capacity plots for the 1st cycle, also apply to the 10th cycle (see Fig. 5). The shape of the three recordings for the electrode made in a mole ratio 1.3, viz. LNMO/Li (Fig. 5a), MCMB/Li (Fig. 5d) and LNMO/MCMB (Fig. 5g), essentially retained the features observed in the first cycle. However, in the cell made in a mole ratio of 2 at the 10th cycle, the singular peak observed close to 0.0 V for the anode (Fig. 5e) and above 4.8 V for the cathode (Fig. 5h) was stronger. Interestingly, the electrochemical response of the spinel versus Li was hardly affected. All these results support the assumption that failure of the cell is caused by a secondary reaction undergone by carbon. Based on previous studies on lithium cells [28,35] such a reaction may be the deposition of Li metal in the MCMB at a late stage of charging. As stated above, the extent of this reaction increases with increasing amount of LNMO spinel in the electrode. This means that lithium plating of the anode is favored in the presence of a large spinel excess, which was the case with a mole ratio of 2. Therefore, ensuring good performance from the Li-ion cell requires careful control of the cathode/anode ratio. On the other hand, this side reaction may explain the increase in delivered capacity with increase in LNMO content and be responsible for the excess capacity observed in MCMB (theoretically, 372 mAh g^{-1}) (see Fig. 3b).

Once some cell construction parameters were optimized, we examined the ability of the cell to operate at higher rates (for example 1C). This was the highest rate at which MCMB exhibited acceptable performance. Fig. 6 shows the capacity delivered by the LNMO/MCMB battery made in a mole ratio of 1.3. As can be seen, the cell performed well in terms of both delivered capacity

(260 Ah kg^{-1}) and capacity retention. The shape of capacity plot for the first cycle was similar to that obtained at C/4, consistent with the reversible process of lithium extraction and insertion (see the inset in Fig. 6).

Our cell has a better capacity retention than that described by Lee et al. [18], even operating at higher rate, 1C versus C/2. The capacity fading in the first 20 cycles was about 15%, lower than that found in the cell without SEI additives reported in Ref. [18] (20%). The use of LiBOB together with the nanosize nature of our spinel could account for this difference.

4. Conclusions

In summary, using the spinel $LiNi_{0.5}Mn_{1.5}O_4$ as cathode and MCMB as anode allows high-energy rechargeable lithium-ion batteries to be made. The use of LiBOB instead of the more common $LiPF_6$ as electrolyte component ensures more efficient capacity retention on cycling. The potential release of HF traces may be the origin of this result. Other cell properties (specifically, the charge/discharge rate and the mole cathode/anode ratio) are governed by the anode material. The use of excess spinel results in Li plating of the anode and in cell degradation as a consequence. The low mole ratio of the cathode and anode is an additional advantage of this Li-ion laboratory cell with a view to obtain high specific energy and power values.

Acknowledgements

This work was supported by CICyT (Project MAT2005-03069) and Junta de Andalucía (Group FQM 175 and Project FQM-01647). The authors thank to Dr. Jan-Christopher Panitz of Chemetall for the LiBOB salt and Mr. Masaki Yamaguchi of Osaka Gas Chemical for the MCMB. We also acknowledge to the reviewers for their valuable comments and suggestions for the improvement of the paper.

References

[1] M. Nishizawa, R. Hashitani, T. Itoh, T. Matsue, I. Uchida, Electrochem. Solid-State Lett. 1 (1998) 10.
[2] G.X. Wang, J. Yao, H.K. Liu, Electrochem. Solid-State Lett. 7 (2004) A250.
[3] J. Yao, G.X. Wang, J.H. Ahn, H.K. Liu, S.X. Dou, J. Power Sources 114 (2003) 292.
[4] J.M. Tarascon, D. Guyomard, J. Electrochem. Soc. 138 (1991) 2864.
[5] Z. Cheng, K. Amine, J. Electrochem. Soc. 153 (2006) A316.
[6] I. Belharouak, Y.K. Sun, W. Lu, K. Amine, J. Electrochem. Soc. 154 (2007) A1083.
[7] M. Sano, T. Hattori, T. Hibino, M. Fujita, Electrochem. Solid-State Lett. 10 (2007) A270.
[8] J.C. Arrebola, A. Caballero, L. Hernán, Nanotechnology 28 (2007) 295705.
[9] R. Benedek, M.M. Thackeray, Electrochem. Solid-State Lett. 9 (2006) A265.
[10] J.W. Jiang, J.R. Dahn, Electrochem. Solid-State Lett. 6 (2003) 180.
[11] K. Xu, S. Zhang, T.R. Jow, Electrochem. Solid-State Lett. 8 (2005) A365.
[12] K. Xu, S.S. Zhang, U. Lee, J.L. Allen, T.R. Jow, J. Power Sources 146 (2005) 79.
[13] Q. Zhong, A. Bonakdarpour, M. Zhang, Y. Gao, J.R. Dahn, J. Electrochem. Soc. 144 (1997) 205.
[14] Y.K. Sun, Y.S. Lee, M. Yoshio, K. Amine, Electrochem. Solid-State Lett. 5 (2002) A99.
[15] J.H. Kim, S.T. Myung, C.S. Yoon, S.G. Kang, Y.K. Sun, Chem. Mater. 16 (2004) 906.
[16] J.C. Arrebola, A. Caballero, M. Cruz, L. Hernán, J. Morales, E. Rodriguez Castellón, Adv. Funct. Mater. 16 (2006) 1904.
[17] Y. Talyosef, B. Marskovski, R. Lavi, G. Salitra, D. Aurbach, D. Kovacheva, M. Gorova, E. Zhecheva, R. Stoyanova, J. Electrochem. Soc. 154 (2007) A682.
[18] H. Lee, S. Choi, H.J. Kim, Y. Choi, S. Yoon, J.J. Cho, Electrochem. Commun. 9 (2007) 801.
[19] J. Hassoun, S. Panero, P. Reale, B. Scrosati, Int. J. Electrochem. Sci. 1 (2006) 110.
[20] G. Armstrong, A.R. Armstrong, P.G. Bruce, P. Reale, B. Scrosati, Adv. Mater. 18 (2006) 2597.
[21] A. Caballero, M. Cruz, L. Hernán, M. Melero, J. Morales, E. Rodríguez Castellón, J. Power Sources 150 (2005) 192.
[22] A. Caballero, M. Cruz, L. Hernán, M. Melero, J. Morales, E. Rodríguez Castellón, J. Electrochem. Soc. 152 (2005) A552.
[23] S. Wang, W. Qiu, T. Li, B. Yu, H. Zhao, Int. J. Electrochem. Sci. 1 (2006) 250.
[24] B. Yu, W. Qiu, F. Li, L. Cheng, J. Power Sources 166 (2007) 499.
[25] C.R. Sides, N. Li, C.J. Patrissi, B. Scrosati, C.R. Martin, MRS Bull. 27 (2002) 604.
[26] A.S. Arico, P. Bruce, B. Scrosati, J.M. Tarascon, W. Schalkwijk, Nature 4 (2005) 366.
[27] F.F.C. Bazito, R.M. Torresi, J. Brazil. Chem. Soc. 17 (2006) 627.
[28] S.S. Zhang, K. Xu, R. Jow, J. Power Sources 160 (2006) 1349.
[29] B.A. Johnson, R.E. White, J. Power Sources 70 (1998) 48.
[30] Z. Chen, W.Q. Lu, J. Liu, K. Amine, Electrochim. Acta 51 (2006) 3322.
[31] K. Amine, J. Liu, S. Kang, I. Belharouak, Y. Hyung, D. Vissers, G. Henriksen, J. Power Sources 129 (2004) 14.
[32] L. Larush-Asraf, M. Biton, H. Teller, E. Zinigrad, D. Aurbach, J. Power Sources 174 (2007) 400.
[33] K. Ariyoshi, Y. Iwakoshi, N. Nakayama, T. Ohzuku, J. Electrochem. Soc. 151 (2004) 296.
[34] T. Terada, K. Yasaka, F. Nishikawa, T. Konishi, M. Yoshio, I. Nakai, J. Solid State Chem. 156 (2001) 286.
[35] J. Fan, S. Tan, J. Electrochem. Soc. 153 (2006) A1081.